Magnetic Fields in Molecular Clouds

Paolo Padoan[1] Tuomas Lunttila[2], Mika Juvela[2], Åke Nordlund[3], David Collins[4], Alexei Kritsuk[4], Michael Normal[4], and Sergey Ustyugov[5]

[1]ICREA & ICC, University of Barcelona, Marti i Franquès 1, E-08028 Barcelona, Spain
email: `ppadoan@icc.ub.edu`

[2]Department of Physics, University of Helsinki, Helsinki, Finland

[3]Niels Bohr Institute, University of Copenhagen, Denmark

[4]CASS / Department of Physics, University of California, San Diego, USA

[5]Keldysh Institute of Applied Mathematics, Russian Academy of Sciences, Moscow, Russia

Abstract. Supersonic magneto-hydrodynamic (MHD) turbulence in molecular clouds (MCs) plays an important role in the process of star formation. The effect of the turbulence on the cloud fragmentation process depends on the magnetic field strength. In this work we discuss the idea that the turbulence is super-Alfvénic, at least with respect to the cloud mean magnetic field. We argue that MCs are likely to be born super-Alfvénic. We then support this scenario based on a recent simulation of the large-scale warm interstellar medium turbulence. Using small-scale isothermal MHD turbulence simulation, we also show that MCs may remain super-Alfvénic even with respect to their rms magnetic field strength, amplified by the turbulence. Finally, we briefly discuss the comparison with the observations, suggesting that super-Alfvénic turbulence successfully reproduces the Zeeman measurements of the magnetic field strength in dense MC clouds.

Keywords. ISM: kinematics and dynamics, MHD, stars: formation, turbulence

1. Star Formation and Supersonic Turbulence

What are the physical processes that determine the mass distribution and the formation rate of stars? We know that stars originate from the gravitational collapse of prestellar cores, but gravity alone cannot determine the wide range of stellar masses, nor the slow rate of star formation. Stellar masses span the approximate range 0.01-100 $m_\odot$ and the most numerous stars have a mass $\ll 1$ $m_\odot$, while the gravitational instability sets a characteristic Jeans mass of 1-10 $m_\odot$ in molecular clouds (MCs). Star-forming gas is converted into stars at a rate of approximately 2% per free-fall time (Krumholz & Tan 2007), while gravity alone would cause the collapse of all gas in one free-fall time.

The observed random velocities in MCs carry a kinetic energy comparable to the cloud gravitational energy, thus turbulence and self-gravity are of comparable importance on scales of several parsecs. Assuming uniform density, the gravitational energy scales as L^2, while the turbulent energy scales as $L^{0.4-0.5}$, based on observations (Larson 1981; Heyer & Brunt 2004; Padoan *et al.* 2006) and simulations (Kritsuk *et al.* 2007; Kritsuk *et al.* 2009). On the average, the turbulent energy must therefore exceed the gravitational energy within a MC, increasingly so towards smaller scales. As shown by Rosolowsky *et al.* (2008), the virial parameter (ratio of turbulent to gravitational energies) in molecular clouds is almost everywhere much larger than unity, except in some of the densest regions. The turbulence is thus able to regulate the star formation rate to a level much lower

than that set by gravity alone (Krumholz & McKee 2005, Padoan & Nordlund 2010, in preparation).

The supersonic turbulent flows in MCs result in a complex network of interacting shocks responsible for the observed filamentary structure. Such flows can naturally assemble dense cores spanning the mass range of stars, suggesting that the turbulence can be directly responsible for the origin of the stellar mass distribution (Padoan & Nordlund 2002; Padoan *et al.* 2007). Although individual prestellar cores eventually collapse into stars due to their own gravity, the initial conditions for the gravitational collapse, specifically the total mass brought into the collapsing region, may be determined by the turbulent flow with little cooperation from the local gravitational force.

Having recognized the importance of turbulence in the fragmentation of MCs, we must establish its nature with respect to the magnetic field strength. How strong is the magnetic field in MCs?

2. The Magnetic Field Strength in MCs

The idea that MCs are magnetically supported against their gravitational collapse is reviewed in Shu *et al.* (1987). In that scenario, the observed random velocities correspond to MHD waves, or perturbations of a strong mean field. Gravitationally bound prestellar cores are initially subcritical and contract because of ambipolar drift until they become supercritical and collapse. Padoan & Nordlund (1997, 1999) investigated the possibility that the mean magnetic field in molecular clouds is weak and the observed turbulence is super-Alfvénic. By comparing results of two simulations, one with a weak field and the other with a strong field, with observational data, they showed that the super-Alfvénic case reproduced the observations better. Further results in support of the super-Alfvénic scenario were presented in Padoan *et al.* (2004) and, more recently, by Lunttila *et al.* (2008) and Lunttila *et al.* (2009), based on simulated Zeeman measurements.

In the following sections, we first address the super-Alfvénic nature of the turbulence in MCs in the context of their formation process. We then present results of large-scale multiphase MHD simulations of driven turbulence to illustrate the origin of the weak mean magnetic field in MCs. Finally, we discuss results of small-scale isothermal MHD turbulence simulations to show that MC turbulence may remain super-Alfvénic even with respect to their rms magnetic field, amplified by the turbulence.

3. Why Are MCs Born Super-Alfvénic?

Skipping a detailed discussion of the different processes that may contribute to the formation of MCs, and entirely neglecting the issue of turning atomic gas into molecules, one can at least say that MCs must be the result of large scale compressions of the warm interstellar medium (WISM). When such compressions reach the pressure threshold of the thermal instability, the compressed gas rapidly cools and compresses further to a characteristic mean density of MCs. This process may be driven, for example, by the evolution of supernova remnants. Irrespective of the specific driving mechanism, we can characterize the large-scale turbulence of the WISM based on its rms sonic and Alfvénic Mach numbers, M_s and M_a. It is generally believed that the large-scale turbulence in the WISM is transonic and trans-Alfvénic, meaning $M_s \sim 1$ and $M_a \sim 1$. This WISM turbulence regime is the fundamental reason why MCs are born super-Alfvénic.

Because of the transonic nature of the WISM turbulence, the large-scale velocity field can occasionally cause compressions strong enough to bring large regions above the thermal instability threshold (this is more likely within spiral arms, where the mean gas
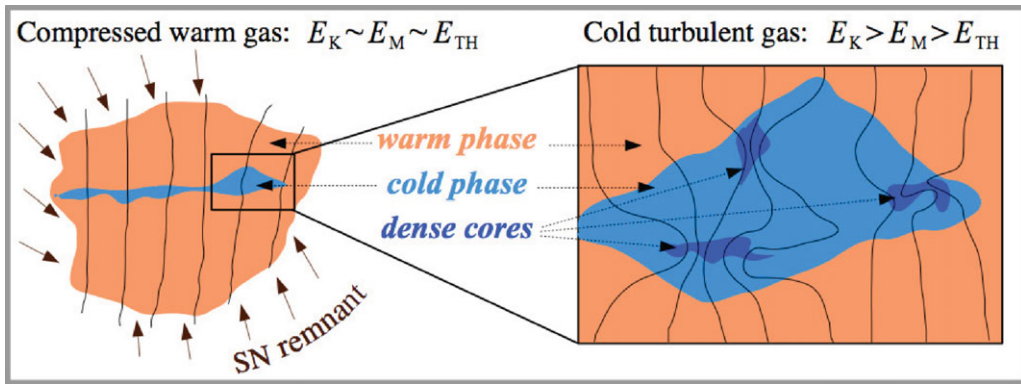
Figure 1. Schematic scenario of the formation of super-Alfvénic MCs.

density has been increased by a spiral arm shock). As the gas is further compressed thanks to its cooling, the magnetic field cannot be compressed because of the initially trans-Alfvénic nature of the flow. In other words, the mean magnetic field is strong enough that the initial compression is forced to be primarily along the magnetic field. Assuming that turbulent velocities are not significantly decreased, the characteristic increase in density, $\rho_{\rm cold} \sim 100 \rho_{\rm warm}$, results in a comparable increase in turbulent kinetic energy, $E_{\rm K,cold} \sim 100 E_{\rm K,warm}$, or a corresponding drop in the rms Alfvén velocity, $V_{\rm a,cold} \sim V_{\rm a,warm}/10$. As a consequence, the turbulence in the rapidly cooling gas must be initially super-Alfvénic with respect to the mean magnetic field. Compression and stretching in this super-Alfvénic flow can then locally amplify the magnetic field, but the mean field (averaged over the whole MC) cannot change much, because the large-scale compressive flow was initially directed to be primarily along the mean magnetic field direction. Because of the reduced temperature, the turbulence in the cold gas is also supersonic, so dense cores with enhanced magnetic field strength are naturally formed by shocks in the turbulent flow. This sequence of events is schematically depicted in Figure 1.

The prediction of a weak mean magnetic field in MCs is further supported by a numerical simulation discussed in the next section. Despite the low mean field, the rms value of B (or the magnetic energy) within MCs is expected to grow due to compression and stretching in the super-Alfvénic flow, and possibly also due to the action of a turbulent dynamo. The evolution of the rms B is investigated in the section after the next one.

4. The Mean B: Large-Scale Multiphase Simulations

In order to test the validity of our general argument about the super-Alfvénic nature of MCs with respect to their mean magnetic field, we have developed a simulation on a numerical mesh of 512^3 computational cells, reproducing global properties of the WISM turbulence. The simulation assumes a mean density of $n_0 = 5$ cm^{-3}, and drives the turbulence to the rms Mach number values of $M_{\rm s} \approx 1.8$ and $M_{\rm a} \approx 0.6$ with respect to the warm phase. The turbulent pressure fluctuations keep 49% of the gas mass and 6% of its volume in the cold phase, while 5% of the mass and 24% of the volume remains in the warm phase. The rest of the gas is found at intermediate temperatures that would be considered thermally unstable in the absence of turbulent pressure. The mean magnetic field strength in the simulation is $B_0 = 3.2$ μG, with an rms value of the same order. The parameters of this simulation may characterize a slightly over-dense region of the ISM

within a spiral arm, on a scale of approximately 200 pc. Details of the simulation will be presented in Kritsuk *et al.* (2010, in preparation). Here we only report some preliminary results on the magnetic field strength.

The left panel of Figure 2 shows the projected density from a snapshot of the simulation. If the box size is assumed to be $L = 200$ pc, filamentary dense regions of length up to approximately 40 pc are common. These are regions of cold gas with a mean density of approximately 100 cm^{-3} and mass up to several thousands solar masses, characteristic values for MCs. We collect a sample of these cold clouds by selecting spatially connected regions within isodensity contours corresponding to $n > 30$ cm^{-3}. We compute the volume-averaged magnetic field strength within each cloud, and plot its distribution on the right panel of Figure 2, as a black histogram. The distribution of the mean magnetic field strength in the clouds is found to peak at 5 μG, less than a factor of two larger than the mean field of the simulation, and covers the approximate range of 0.5-10 μG. This result confirms that approximately transonic and trans-Alfénic turbulence in a gas with the cooling properties of the WISM naturally generates dense regions of cold gas with global properties characteristic of MCs and mean magnetic field strength only a little larger than the large scale mean value in WISM.

The right panel of Figure 2 shows also the histograms of B for all computational cells with $n < 2$ cm^{-3} and with $n > 30$ cm^{-3}. Values much larger than the mean can be found in both histograms, but particularly so in the case of the dense and colder gas. That is because, as explained in the previous section, the turbulence is super-Alfvénic and supersonic in the cold gas, so large enhancements of both B and n are expected within the cold clouds. The magnetic field distribution in the cold gas shows a very extended exponential tail, as in isothermal simulations of super-Alfvénic turbulence (Padoan & Nordlund 1999). However, the average field within each cloud remains rather weak (see black histogram), as argued in the previous section.

Although the turbulence within the largest clouds in the simulation is super-Alfvénic, their value of M_a is under-estimated due to the limited numerical resolution. A much larger resolution is needed to resolve well the internal cloud turbulence. This should not affect the derived mean magnetic field strength in the clouds, but it is certainly a significant numerical limitation with respect to the evolution of the cloud rms B. In order to study the evolution of the rms B within regions of cold gas, we focus in the next section on simulations of isothermal super-Alfvénic turbulence.

5. The rms B: Small-Scale Isothermal Simulations

If their super-Alfvénic turbulence generates a dynamo, MCs with a very weak mean magnetic field may in principle have their magnetic energy amplified to equipartition with the turbulent kinetic energy. If that were achieved during their lifetime, MCs that are born (and remain) super-Alfvénic with respect to their mean magnetic field, may evolve to become trans-Alfvénic at least with respect to their rms magnetic field. To investigate the saturated value of the rms magnetic field strength we have run a set of isothermal MHD turbulence simulations with rms Mach numbers $M_s \approx 10$ and $M_{a,0} \approx 30$, 10, and 3, where $M_{a,0}$ is the rms Alfvénic Mach number with respect to the Alfvén velocity defined with the mean magnetic field, B_0, and the mean gas density, n_0. The turbulence is driven by a random force within the wavenumber range $1 \leqslant k \leqslant 2$ ($k = 1$ corresponds to the computational box size) for several dynamical times, starting from uniform magnetic and density fields. The runs are repeated at three different numerical resolutions, on mesh sizes of 256^3, 512^3, and 1024^3 computational cells. Details about the PPML code and the simulations can be found in Ustyugov *et al.* (2009) and in Kritsuk *et al.* (2009a,b).
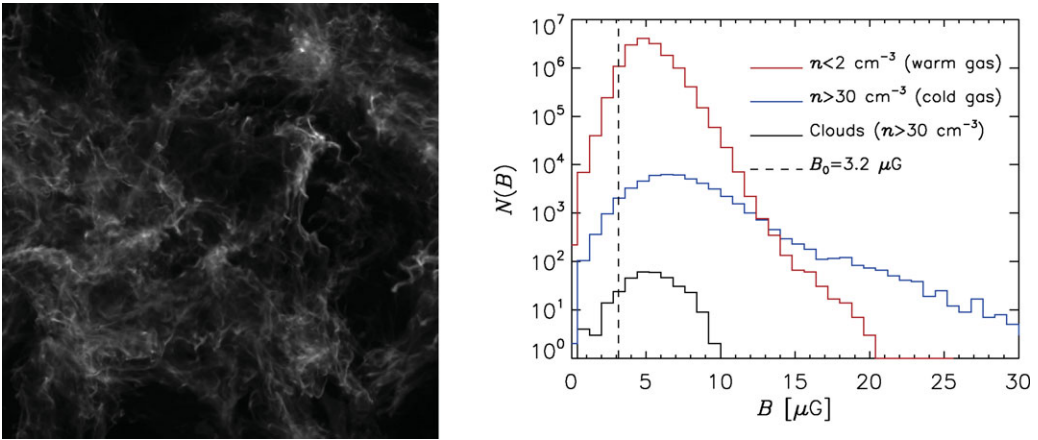
Figure 2. *Left:* Projected density field from the multiphase turbulence simulation representing a region of approximately 200 pc (the grey scale is linearly proportional to the column density). *Right:* Probability distribution of the magnetic field strength in the warm gas (red histogram), the cold gas (blue histogram), and averaged inside MCs (black histogram). The vertical dashed line corresponds to the mean magnetic field in the simulation, $B_0 = 3.2$ μG, representing the mean magnetic field strength in the Galactic disk. The characteristic mean field in MCs is approximately 5 μG, very close to the mean Galactic value.

The non-dimensional parameters of the runs are listed in Table 1, where β_0 is the ratio of gas to magnetic pressure, $\beta_0 = 2(M_{a,0}/M_s)^2$, based on the mean magnetic field and the mean density. The two last columns of Table 1 give the saturated rms values of the Alfvénic Mach number and of the ratio of gas to magnetic pressure, M_a and β, after the rms field has been amplified to saturation. Based on those values of M_a, one can see that only the simulation with the strongest mean magnetic field becomes trans-Alfvénic with respect to the rms magnetic field.

The time evolution of magnetic and turbulent kinetic energy is plotted in Figure 3, with the energy shown with linear and logarithmic scales on the left and right panels respectively. The magnetic energy is amplified and reaches saturation after approximately three dynamical times. The amplification can be entirely accounted for by a combination of compression and stretching events. There is no evidence of a real turbulent dynamo, meaning constructive twisting and folding events that could further amplify the magnetic field. In the simulation with the weakest mean magnetic field there is a very slow field amplification during most of the evolution. Even if that were due to a turbulent dynamo, the growth rate would be extremely low and the effect of the turbulent dynamo irrelevant within a MC lifetime. Only the simulation with the strongest mean magnetic field reaches equipartition of kinetic and magnetic energy, while in the other two runs the magnetic energy remains approximately 4 and 10 times smaller than the turbulent kinetic energy.

The saturation level of the rms magnetic field strength could depend on numerical resolution. By performing a numerical convergence test, we have verified that at a resolution of 1024^3 computational cells the saturation level of the magnetic energy is almost converged. Dynamo action may also depend on the magnetic Prandtl number, P_m, giving the ratio of viscosity and resistivity, $P_m = \nu/\eta$. In numerical simulations where the resistivity and viscosity are not explicitly included, the effective value of P_m is of order unity. In real MCs it is many orders of magnitude larger. The turbulence regime with a value of P_m as large as in MCs cannot be tested numerically. However, previous numerical work by Haugen *et al.* (2004) suggests that the growth rate of the turbulent dynamo in the
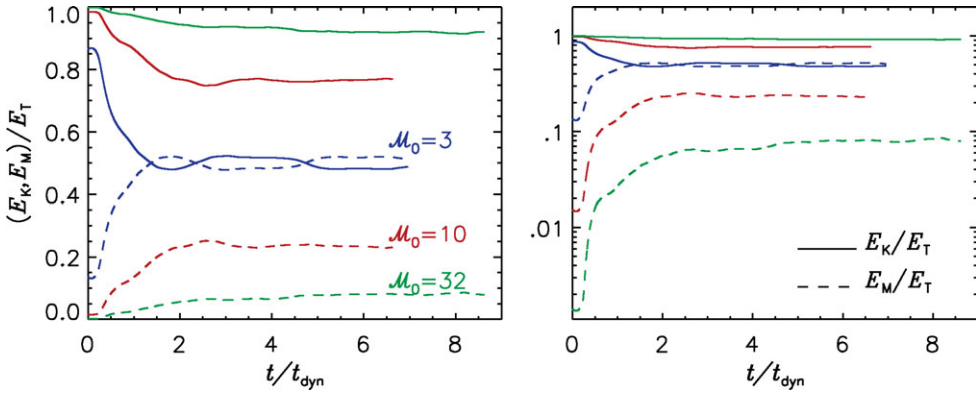
Figure 3. *Left:* Time evolution of magnetic and kinetic energies (normalized to the total energy), in the three 512^3 runs with different values of B_0. The energy scale is linear *Right:* Same as the left panel, but with a logarithmic energy scale to show better the magnetic energy amplification in the run with the weakest mean magnetic field.

| Based on B_0 and n_0:			Saturated values:	
M_{s}	$M_{\mathrm{a},0}$	β_0	M_{a}	β
10	31.6	20.0	9.2	0.11
10	10.0	2.0	3.0	0.03
10	3.2	0.2	1.1	0.01

Table 1. Non-dimensional parameters of the isothermal MHD turbulence simulations.

supersonic regime may be significantly reduced. It is possible that when gas elements of a supersonic turbulent flow dissipate their energy in shocks, their ability to twist and fold constructively is largely reduced compared to the case of fluid elements following the vortical motions of an incompressible turbulent flow.

Taking our numerical results at face value, we would conclude that MCs may remain super-Alfvénic also with respect to their rms magnetic field strength over their whole lifetime. Only MCs that are born with a relatively strong mean magnetic field may have a chance to reach equipartition of kinetic and magnetic energies. However, equipartition is always rapidly reached locally. The magnetic pressure in the postshock regions has to balance the gas ram pressure, which is the same in three runs, because $M_{\mathrm{s}} \approx 10$ in all of them. The largest values of B, typically found in the densest regions, are thus weakly dependent on the mean or rms magnetic field strength.

5.1. $B - n$ correlation in super-Alfénic turbulence

In super-Alfvénic turbulence, the local magnetic field strength correlates with the gas density, as long as the turbulence remains super-Alfvénic with respect to both the mean and the rms magnetic field strength. Figure 4 shows scatter plots of magnetic versus gas pressure in the case of the run with the largest value of B_0, where the magnetic energy has reached equipartition with the turbulent kinetic energy (left panel), and in the case of the lowest value of B_0, which is still super-Alfvénic also with respect to the rms magnetic field strength (right panel). In the strong B_0 case there is almost no $B - n$ correlation. This would be even more true in the case of a trans-Alfvénic run with respect to the mean magnetic field (Padoan & Nordlund 1999). In the weak B_0 case, despite the large scatter, there is a clear trend of increasing B with increasing n. The
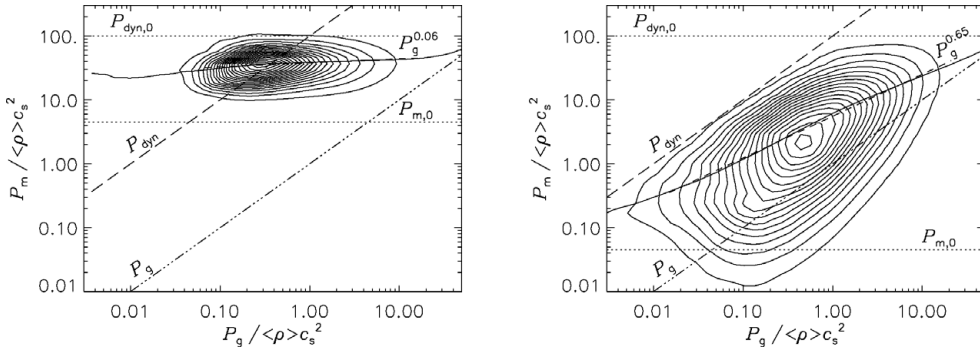
Figure 4. *Left:* Scatter plot of magnetic versus gas pressures, normalized to the mean gas pressure, for the case with the strongest mean magnetic field strength, $M_{a,0} = 3$. The top dotted line shows the characteristic value of the dynamic pressure, defined with the mean density and the global rms velocity. The bottom dotted line corresponds to the value of the mean magnetic pressure. The diagonal dashed line is the dynamic pressure defined with the global rms velocity and the local density. The diagonal dashed-dotted line is the local gas pressure. The solid line shows the mean magnetic pressure as a function of gas pressure. The power law fit gives $P_m \propto P_g^{0.06}$ *Right:* Same as on the left panel, but for the simulation with $M_{a,0} = 32$. The mean magnetic pressure increases with gas pressure following approximately a power law, $P_m \propto P_g^{0.65}$.

mean value of magnetic pressure grows with gas pressure approximately as a power law, $P_m \propto P_g^{0.65}$, corresponding to $B \propto n^{0.32}$. The upper envelope of the scatter plot shows that, at each density, the largest values of magnetic pressure scale approximately as the dynamic pressure defined with the global rms velocity and the local density. While the magnetic pressure is almost always in excess of the gas pressure, it almost never exceeds the dynamic pressure defined above, showing that the magnetic field plays primarily a passive role in the dynamics. In the strong B_0 case, instead, the magnetic pressure often exceeds the dynamic pressure.

6. Comparison with Observations

Padoan & Nordlund (1999) discussed several observational tests of numerical simulations of supersonic MHD turbulence that could be used to constrain the mean magnetic field. Based on those tests, they suggested that turbulence in MCs is super-Alfvénic with respect to their mean magnetic field on scales of few to several parsecs. This super-Alfvénic model of star-forming regions was recently used to generate simulated measurements of the Zeeman effect on 18 cm OH lines (Lunttila *et al.* 2008). It was shown that a super-Alfvénic turbulence simulation with the characteristic size, density, and velocity dispersion of star-forming regions could produce dense cores with the same $|B_{los}|$-N relation as observed cores. Lunttila *et al.* (2008) also computed the relative mass-to-flux ratio $\mathcal{R}_\mu$, defined as the mass-to-flux ratio of a core divided by that of its envelope, following the observational procedure proposed by Crutcher *et al.* (2009). They found a large scatter in the value of $\mathcal{R}_\mu$, and an average value of $\mathcal{R}_\mu < 1$, in contrast to the ambipolar-drift model of core formation, where the mean magnetic field is stronger and only $\mathcal{R}_\mu > 1$ is allowed. The observational results of Crutcher *et al.* (2009) confirmed $\mathcal{R}_\mu < 1$ in observed cores, as predicted by Lunttila *et al.* (2008) for the super-Alfvénic model.

Here we present further evidence that the same super-Alfvénic simulation compares well with the observational data, summarizing the main results of Lunttila *et al.* (2009).
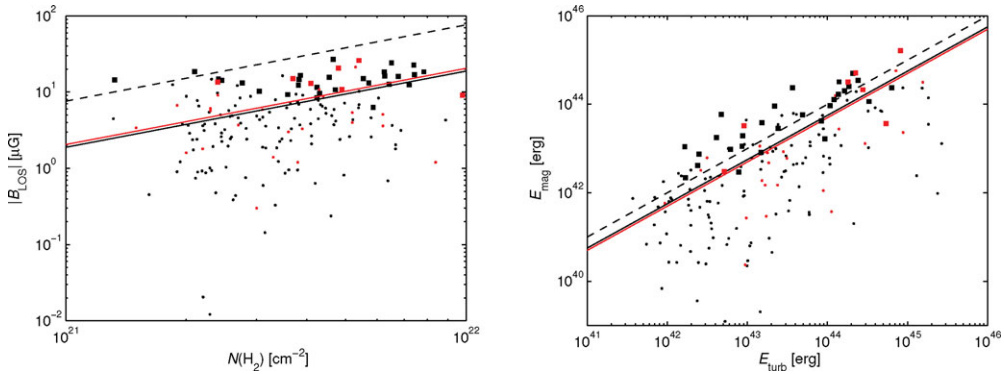
Figure 5. *Left:* Inferred line-of-sight magnetic field as a function of H_2 column density. Black symbols show the results from our simulation, red symbols are cores from Troland & Crutcher (2008). Squares show 3σ detections, and dots are non-detections. The black solid line shows the mean mass-to-flux ratio of the simulated cores, and the red solid line the mean mass-to-flux ratio calculated from Troland & Crutcher (2008) observations. The dashed line is the critical mass-to-flux ratio with no geometrical correction, $\lambda = 1$. *Right:* Magnetic energy versus turbulent kinetic energy for the same cores and with the same symbols as in the left panel. The dashed line corresponds to the energy ratio $\beta_{\mathrm{turb}} = E_{\mathrm{turb}}/E_{\mathrm{mag}} = 1$. The solid black line shows the mean energy ratio for the simulated cores, and the red solid line for Troland & Crutcher (2008) observations.

Lunttila *et al.* (2009) used simulated OH Zeeman measurements to compute the mass-to-flux ratio relative to the critical one, λ, and the ratio of turbulent to magnetic energies, β_{turb}, in molecular cores selected from simulated maps. They followed closely the observational procedure of Troland & Crutcher (2008), and found mean values of λ and β_{turb} in good agreement with the observational results.

The work of Lunttila *et al.* (2009) is based on a simulation run on a mesh of 1000^3 zones with the Stagger Code Padoan *et al.* (2007), with periodic boundary conditions, isothermal equation of state, random forcing in Fourier space at wavenumbers $1 \leqslant k \leqslant 2$ ($k = 1$ corresponds to the computational box size), uniform initial density and magnetic field, and random initial velocity field with power only at wavenumbers $1 \leqslant k \leqslant 2$. The rms sonic Mach number is $\mathcal{M}_s = \sigma_{v,3D}/c_s = 8.91$. The initial and evolved rms Alfvénic Mach numbers are $M_{a,0} = 29.7$ and $M_a = 2.8$ respectively.

For the computation of synthetic Zeeman spectra the data cube was scaled to physical units, assuming $L = 9$ pc, $\langle n(H_2) \rangle = 67$ cm^{-3} (typical for that scale in the sample of Falgarone *et al.* (1992)), and $T_{\mathrm{kin}} = 10$ K. A constant fractional OH abundance of $[\mathrm{OH}]/[\mathrm{H}] = 4.0 \times 10^{-8}$ was assumed, following Crutcher (1979). Radiative transfer calculations were performed to compute simulated Zeeman measurements of the 1665 and 1667 MHz OH lines observed by Troland & Crutcher (2008). The synthetic observations were made with a 3 arcmin (fwhm) beam, corresponding to the angular resolution of the Arecibo telescope, and using a channel separation of 0.05 km s^{-1}.

In order to compare the simulations with the observations of Troland & Crutcher (2008), dense cores were selected from the OH emission position-position-velocity data cubes using the clumpfind algorithm of Williams *et al.* (1994). Before applying the clumpfind routine, the data cubes were resampled to an angular resolution of ~ 1.2 arcmin (approximately Nyquist sampled), and uncorrelated Gaussian noise with rms of 0.08 K was added to simulate observational noise.

Core physical parameters obtained from the simulated observations agree well with those in the sample of Troland & Crutcher (2008). In particular, the mean values of the

mass-to-flux ratio relative to the critical one, λ, and of the ratio of turbulent to magnetic energies, β_{turb} are $\langle\lambda\rangle_{\text{sim}} = 3.9$ and $\langle\beta_{\text{turb}}\rangle_{\text{sim}} = 1.8$, almost identical to those from the observed core sample, $\langle\lambda\rangle_{\text{obs}} = 3.8$ and $\langle\beta_{\text{turb}}\rangle_{\text{obs}} = 1.9$. As shown in Figure 5, also the scatter around these mean values found in the observations is reproduced well by the simulated cores. Even using only detections, both observed and simulated cores appear to be supercritical, while their turbulent kinetic energy is of the order of their magnetic energy, but with a significant scatter.

If the MC turbulence is indeed super-Alfvénic, the scatter found around the mean values of λ and β_{turb} is only partly due to the random orientation of the magnetic field with respect to the line of sight (the Zeeman measurements are only sensitive to the line-of-sight component of the magnetic field). Part of the scatter originates from intrinsic variations of the magnetic field strength from core to core. Such intrinsic variations of magnetic field strength are not expected in the traditional picture of MCs were the mean magnetic field is strong (Shu *et al.* 1987).

7. Conclusions

We have argued that MCs are born super-Alfvénic with respect to their mean magnetic field, because of the trans-Alfvénic nature of the turbulence in the WISM. Using a multiphase turbulence simulation meant to represent an overdense region (spiral arm) of the WISM turbulence on a scale of order 200 pc, we have shown that large regions of cold dense gas are formed by transonic or mildly supersonic large-scale turbulent compressions, with physical properties (mean density, size, and temperature) characteristic of MCs. We have shown that the mean field within these clouds is on the average around 5 μG, only slightly larger than the assumed mean field of 3.2 μG (with a comparable rms). This simulation confirms our general argument about the super-Alfvénic nature of clouds formed out of trans-Alfvénic turbulence in a gas with the cooling properties of the WISM. If large scale turbulence, driven for example by the evolution of SN remnants, plays an important role in their formation, MCs should be born with a rather weak mean magnetic field, as suggested by Padoan & Nordlund (1997, 1999). The actual process of MC formation is of course much more complex, especially with regard to the formation of molecular species.

We have then addressed the question of the time evolution of the rms magnetic field strength, or magnetic energy. Using a set of isothermal simulations of supersonic and super-Alfvénic turbulence, we have shown that magnetic energy can reach equipartition with the turbulent kinetic energy only in the case where the mean field is already not too far from equipartition. If a turbulent dynamo operates at all, beyond the saturated field level reached in the simulation, its growth rate may be too small to be relevant within a MC lifetime. We conclude that a significant fraction of MCs may remain super-Alfvénic also with respect to their rms magnetic field strength.

Despite the small value of their mean magnetic field strength, super-Alfvénic MCs are expected to naturally generate regions of stronger magnetic field, particularly where dense cores are formed. When the gas density is enhanced by turbulent shocks, the magnetic field is also enhanced due to the combined effects of the compression of the field component perpendicular to the shock direction and of the field stretching by the shear flow in the postshock layers. We have shown that the properties of dense MC cores formed in this way in the simulations are consistent with those of real cores observed by Troland & Crutcher (2008). The mean values of the mass-to-flux ratio relative to the critical one, λ, and of the ratio of turbulent to magnetic energies, β_{turb}, are $\langle\lambda\rangle_{\text{sim}} = 3.9$ and $\langle\beta_{\text{turb}}\rangle_{\text{sim}} = 1.8$, almost identical to those from the observational sample, $\langle\lambda\rangle_{\text{obs}} = 3.8$

and $\langle\beta_{\mathrm{turb}}\rangle_{\mathrm{obs}} = 1.9$. The relative mass-to-flux ratio (core to envelope) was predicted to be less than unity in super-Alfvénic turbulence, at least for cores where the magnetic field could be detected, in contrast to the basic ambipolar drift model of core formation, where that ratio was predicted to be larger than unity. Recent observations by Crutcher *et al.* (2009) have confirmed this prediction of the super-Alfvénic model.

Acknowledgements

References

M. R. Krumholz & J. C. Tan, *ApJ* **654**, 304–315 (2007).

R. B. Larson, *MNRAS* **194**, 809–826 (1981).

M. H. Heyer & C. M. Brunt, *ApJL* **615**, L45–L48 (2004).

P. Padoan, M. Juvela, A. Kritsuk & M. L. Norman, *ApJL* **653**, L125–L128 (2006).

A. G. Kritsuk, M. L. Norman, P. Padoan & R. Wagner, *ApJ* **665**, 416–431 (2007).

A. G. Kritsuk, S. D. Ustyugov, M. L. Norman & P. Padoan, *Journal of Physics Conference Series* **180**, 012020 (2009).

E. W. Rosolowsky, J. E. Pineda, J. Kauffmann & A. A. Goodman, *ApJ* **679**, 1338–1351 (2008).

M. R. Krumholz & C. F. McKee, *ApJ* **630**, 250–268 (2005).

P. Padoan & A. Nordlund, *ArXiv e-prints* (2009), `arXiv:astro-ph/0907.0248`.

P. Padoan & Å. Nordlund, *ApJ* **576**, 870–879 (2002).

P. Padoan, Å. Nordlund, A. G. Kritsuk, M. L. Norman & P. S. Li, *ApJ* **661**, 972–981 (2007).

F. H. Shu, F. C. Adams & S. Lizano, *ARA&A* **25**, 23 (1987).

P. Padoan & Å. Nordlund, *ArXiv e-prints* (1997) `arXiv:astro-ph/9706176`.

P. Padoan & Å. Nordlund, *ApJ* **526**, 279 (1999).

P. Padoan, R. Jimenez, M. Juvela & Å. Nordlund, *ApJL* **604**, L49–L52 (2004).

T. Lunttila, P. Padoan, M. Juvela & Å. Nordlund, *ApJL* **686**, L91–L94 (2008).

T. Lunttila, P. Padoan, M. Juvela & Å. Nordlund, *ApJL* **702**, L37–L41 (2009).

S. D. Ustyugov, M. V. Popov, A. G. Kritsuk & M. L. Norman, *Journal of Computational Physics* **228**, 7614–7633 (2009).

A. G. Kritsuk, S. D. Ustyugov, M. L. Norman & P. Padoan, ASPC, 406, 15 (2009)

N. E. L. Haugen, A. Brandenburg, & A. J. Mee, *MNRAS* **353**, 947–952 (2004).

T. H. Troland & R. M. Crutcher, *ApJ* **680**, 457–465 (2008).

E. Falgarone, J. L. Puget & M. Pérault, *A&A* **257**, 715 (1992).

R. M. Crutcher, *ApJ* **234**, 881–890 (1979).

J. P. Williams, E. J. De Geus & L. Blitz, *ApJ* **428**, 693 (1995).

R. M. Crutcher, N. Hakobian & T. H. Troland, *ApJ* **692**, 844–855 (2009).